

# A NOVEL FAÇADE SANDWICH PANEL WITH LOW-DENSITY WOOD FIBRES CORE

José L. Fernández-Cabo<sup>1</sup>, M. Almudena Majano Majano<sup>1</sup>, Luis San-Salvador Ageo<sup>1</sup>, Miguel Ávila Nieto<sup>1</sup>

**ABSTRACT:** The work explores, experimentally and theoretically, the possibility of producing a novel cladding sandwich panel comprised of a low-density wood fibres (WF) core, made with GUTEX®, and timber engineering board faces. A short discussion of the possibility of using thermal treated timber at the outer face is also made.

Tests on small specimens, using physical and optical devices, were performed for the basic mechanical characterization of WF. Shear modulus  $G$  was the main target; and values for a range of nominal densities from  $\rho = 110$  to  $190$  kg/m<sup>3</sup> were obtained.

Short term load tests on real scale WF sandwich (WFS) specimens of 3.2m span were also performed. An initial simple analytical structural model, based on Annex B of Eurocode-5 (CEN-1995, 2003) was used, taking into account the shear deformation of the core.

The results show that WFS's are a viable solution at least for claddings. The line of work is especially attractive as WF is a natural and sustainable product.

This research has been carried out with financial support from the European Community within the Sixth Framework Program (NMP2-CT-2005-IP 011799-2).

**KEYWORDS:** Low-density wood fibres, green composites, sandwich beams

## 1 INTRODUCTION

The development of new building materials and systems based on sustainable and ecological criteria is clearly a current challenge in the building construction field. The design of new claddings is a crucial issue. The development of novel sandwiches presents the advantage of coupling building physics and structural criteria.

Considering non-steady state situations, low density wood fibre (WF) panels also have an advantage over plastic foams and mineral wools. Thanks to their better thermal effusivity, they better stabilize indoor temperatures. As the weight is higher in relation with the alternative solutions in extruded polystyrene (XPS) or rock wool, the acoustics insulation is also increased, a relevant issue nowadays. The porosity of WF translates again into acoustic benefits. WF has of course clear advantages when sustainability criteria are used.

The paper reports the experimental and theoretical work carried out for studying the viability of producing a WF sandwich (WFS) for a novel cladding. Different nominal densities ( $\rho$ ) of WF ranging between 110 to 190 kg/m<sup>3</sup> were used in the tests. This variation of density hardly

affects WF's thermal conductivity value, maintained around 0.04 W/mK; this insulation is in the same range as other existing foam, such as expanded polystyrene (EPS) and XPS. These data explain why the use of WF insulation in building construction is an increasing practice in Europe, especially in Germany and Austria.

In the initial part of the experimental work, the shear modulus ( $G$ ) values of the WF for a range of  $\rho$  from 110 to 190 kg/m<sup>3</sup> were obtained. The bending stiffness of the timber faces were also measured for checking the nominal data. Real scale tests, simulating the wind load, were developed in the second part of the experimental work. The empirical data were quasi-linear, and therefore the results were compared with a simple theoretical linear model. As the experimental and theoretical results agreed reasonably well, a simple parametrical study was developed in order to complement the conclusions.

## 2 MATERIALS AND METHODS

### 2.1 MATERIALS AND PRODUCTION PROCESS OF WFS

WFS specimens were industrially assembled by the company Dold Holzwerke [6]. The faces of the WFS were made of oriented strand boards (OSB) 15 mm thick, and the core was made with GUTEX® WF [10] of four different  $\rho$ : 110, 130, 150 and 190 kg/m<sup>3</sup>. These

<sup>1</sup> José L. Fernández-Cabo, ETS. of Architecture, Structural Department, Technical University of Madrid, Avda. Juan de Herrera 4, 28040 Madrid, Spain. Email: jose.fcabo@upm.es

densities approximately correspond to the following commercial names: Gutex Thermosafe homogeny, Gutex Thermosafe-wd, Gutex Thermowall, Gutex Ultratherm.

The nominal depth of the core was 120 mm. Actual depths varied from 110 to 120 mm due to the pressure applied during the gluing process.

Real scale WFS tests and small scale shear tests were performed using pieces obtained from the same production element in order to reduce material uncertainties. The gluing machine used spreads glue strips along the panel, obtaining a real glued surface that is approximately half of the full contact surface.

## 2.2 SET UP OF SMALL SCALE SHEAR TESTS OF WF

A set up (Fig. 1) similar to the timber standard NT BUILD 378: 1991, considered to be valid for this material, was chosen for the tests. Previous tests were required for determining the breaking load,  $F_{v,max}$ . The  $G$  value is calculated according to a linear relationship between  $0.1 \cdot F_{v,max}$  and  $0.4 \cdot F_{v,max}$ . Displacement control was used, with a rate of 0.25 mm per minute.

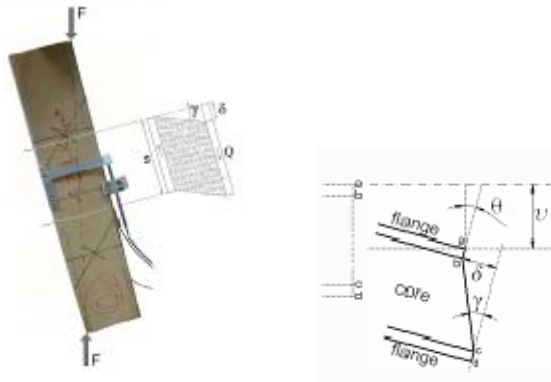


**Figure 1:** Set up for the shear test similar to NT BUILD 378:1991, and degrees of freedom for the basic structural model: deflection ( $v$ ), rotation ( $\theta$ ), and slip deformation of the core ( $\delta$ ).

The upper and lower faces had the same rotation,  $\theta$ , in each section. Due to this, the LVDT of the set up measures the whole slip,  $\delta$ , between the faces, including any possible local slip at the OSB-WF contact surface (whether the variation across the WF section is linear or not). The  $G$  value obtained can be then called global, as it takes into consideration the total slip and not its governing law.

A second measuring procedure involved optical measurements, using ARAMIS® system, with 3D capabilities, and a resolution of 2 mega pixels, was carried out.

## 2.3 BENDING TESTS ON OSB PANELS

The  $EI$  value of the OSB panels was tested in a total of four samples. Two tests were carried out using a three point set up, and a further two using a four point set up. The reason for using two different set ups was to try to

verify the homogeneity of the material. The procedure was similar to EN-310:1993 (which calculates the Young modulus, not  $EI$  as a single value). The span was 1m and the width was the same as that of the original WFS, i.e. approximately 475 mm.

## 2.4 SET UP OF REAL SCALE TEST OF WFS

Bending tests were all carried out for a free span of 3200 mm, using 3400 mm long specimens in a six-point type arrangement (Fig. 2). The technical report EOTA TR002 (EOTA. 2000, Test methods for Light Composite Wood-based Beams and Columns), uses a four-point arrangement. The six-point arrangement was preferred here, at this preliminary stage, for better checking the theoretical model (the bending moment is almost exact to that generated by a uniformly distributed load). Controlled displacement, with a rate of 1 mm per minute, was chosen. With the WF panel thickness of 120mm and the free span of 3200, a standard slenderness ratio of  $3200/(15+120+15)=21.3$  for a façade panel was achieved.

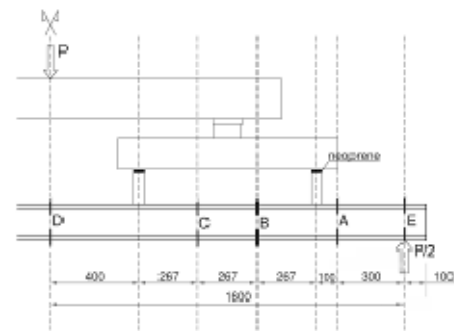


**Figure 2:** General set up and reference sections (only the instrumented half of the beam is shown).

Two groups of tests were performed: the first, referred to as partially instrumented (P-IT), for  $\rho$  of 110 and 130  $\text{kg/m}^3$ , only measured load versus deflection at midspan; and the second set, referred to as globally instrumented (G-IT), for  $\rho$  of 150 and 190  $\text{kg/m}^3$ , performed with a more complete instrumentation and therefore capable of achieving a more refined calibration. The specimens of  $\rho=110 \text{ kg/m}^3$  turned out to be too weak for a span of 3.2 m. They were not easy to test, and this is the main reason why the research quickly focused on the higher densities (150 and 190  $\text{kg/m}^3$ ).

The G-IT group consisted of three further sets of tests done on the same WFS specimen. Set-1 and set-2 were carried out without breaking the sandwich; they stopped when the maximum deflection reached 15mm for  $\rho=190 \text{ kg/m}^3$ , and 10mm for  $\rho=150 \text{ kg/m}^3$ . Set-2 was only added to check vertical movements of the core over the supports. None of the beams broke at set-2. For set-3 the load was increased until fracture occurred.

## 2.5 STRUCTURAL MODEL FOR BENDING

A simple linear model, based on Annex B of Eurocode 5 (EC-5, Annex B) (CEN-1995, 2003), was mainly used, although other sources were also compared, as we shall

see. The proposed WFS clearly belong to the field of timber engineering, and therefore EC-5 was the initial reference. The use of this standard would help in the application of ETAG-016 (part 3) (EOTA 2005). EC-5 model is a linearized model: the stiffness of the connection is linearized using equivalent secant values. The same approach will be used here.

The assumptions are: 1) linear-elastic constitutive equations, 2) the axial stiffness of the core is neglected, 3) the curvature at both flanges is the same, 4) shear deformation is considered only at the core, not at the flanges, 5) the vertical deflection of the two flanges is the same (the kinematic model was shown in Fig. 1). Three degrees of freedom per section are then considered: deflection ( $v$ ), rotation ( $\theta$ ) and slip of the core ( $\delta$ ); which is the typical assumption for sandwich beams with a linear behaviour.

The equivalent bending stiffness of the sandwich beam for a simply supported beam with uniformly distributed load, according to the gamma method of EC-5, is ( $\gamma^*$  is used instead of  $\gamma$ , as in EC-5 Annex B, as the latter is normally reserved for the engineering shear strain):

$$\gamma_i^* = \frac{1}{1 + \frac{\pi^2 \cdot E_i \cdot A_i}{l^2} \cdot \frac{1}{k_{wt,i}}} = \frac{1}{1 + \frac{\pi^2 \cdot E_i \cdot A_i}{l^2} \cdot \frac{h_2}{2 \cdot G_{sec} \cdot b}} \quad (1)$$

$$EI_{eff} = \sum_{i=1,3} (E_i \cdot I_i + \gamma_i^* \cdot E_i \cdot A_i \cdot a_i^2) \quad (2)$$

where  $A_i$  is the area of the individual part -i- (1 and 3),  $l$  the span, and  $a_i$  the distance from the center of gravity of the whole sandwich to the center of gravity of the individual part -i-. The value of  $a_i$  can be, in general, calculated using the EC-5 formulation based on the homogenization of the section.

The shear stresses at the core are (as the core does not bear normal stress, the shear stress across the core is constant):

$$\tau_{core,i} = \frac{\gamma_i^* \cdot E_i \cdot A_i \cdot a_i \cdot V}{EI_{eff} \cdot b} \quad (3)$$

where  $V$  is the shear force,  $b$  the width of the core, i.e. the width of the sandwich, and -i- 1 or 3.

### 3 RESULTS

#### 3.1 SHEAR MODULUS OF THE WF CORE

Optical measurements were able to reflect the whole slip across five sections of the WF cores separated around 20mm. The non linear law reflected the variation of density across the section. It was confirmed that no noticeable local slip took place at the OSB-WF interface.

It is worth mentioning that the bigger the density, the smaller the variation of density across the section. Considering the full slip between OSB faces,  $G$  is a quasi-linear parameter. The linearized  $G_{sec}$  values adopted, calibrated using the results of the real scale tests, are shown in the Table 1.

**Table 1:** Equivalent secant shear modulus,  $G_{sec}$  (N/mm<sup>2</sup>), and shear strength,  $f_{v,sec}$  (N/mm<sup>2</sup>), for four different densities (kg/m<sup>3</sup>)

$\rho$	110	130	150	190
$G_{sec}$	0.7	1.06	3.3	5.9
$f_{v,sec}$	0.0077	0.0133	0.054	0.096

Table 1 also summarizes the values of shear secant strength,  $f_{v,sec}$ , for the four analysed densities. The values were derived from the breaking load of the real scale test together with the theoretical model.

#### 3.2 BENDING STIFFNESS EI OF THE OSB PANELS

The  $EI$  value was obtained specifically for checking the nominal  $EI$  value of the OSB panels produced by Kronofrance, given to be  $EI=1.9125$  kNm<sup>2</sup>/m. An average value of  $EI=2.29$  kNm<sup>2</sup>/m, derived from the test, was used in the calculations.

#### 3.3 EMPIRICAL DATA VERSUS ANALYTICAL MODEL: DEFLECTION

The following figure (Fig. 3) plot the total force (kN) versus the deflection (dotted lines) at sections B and C recorded in the tests (Fig. 2). It is compared the empirical data using a linear regression plot (dashed line), a typical curve (dotted lines), and the theoretical EC-5 model (continuous line), for  $\rho=150$  and  $190$  kg/m<sup>3</sup>,

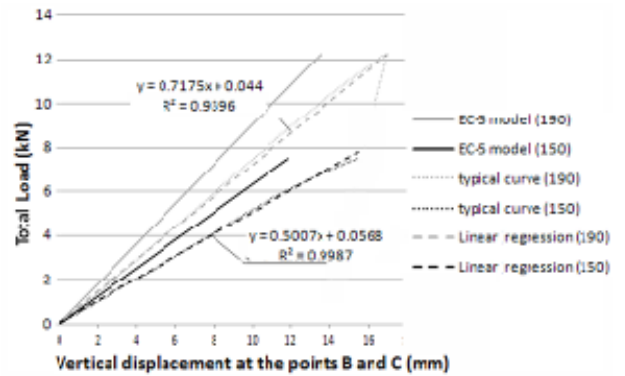


**Figure 3:** Total load (kN) versus deflection (mm) at points B and C (see Fig. 2) for  $\rho_{nom}=150$  and  $190$  kg/m<sup>3</sup>

#### 3.4 EMPIRICAL DATA VERSUS ANALYTICAL MODEL: TOTAL SLIP AT THE CORE

The total force (kN) versus the slip at the core was also plot (Fig. 4). It is shown the comparison between the empirical data (dashed line), typical curve (dotted lines), and the theoretical EC-5 (continuous line), for  $\rho=150$  and  $190$  kg/m<sup>3</sup>, at sections B and C (see Fig. 2), where the shear force is equal. The point selected in the linear model for the comparison was the middle point between

B and C, as the shear force at this point in the model is equal to the shear force in the test at B and C.

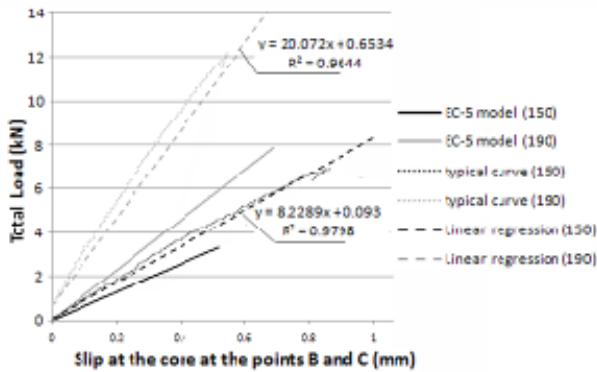


**Figure 4:** Total load (kN) versus total slip at the core (mm) at points B and C (see Fig. 3) for  $\rho_{nom}=150$  and  $190 \text{ kg/m}^3$

### 3.5 EMPIRICAL DATA VERSUS ANALYTICAL MODEL: ROTATIONS

Figs 5a and 5b show the comparison between the empirical data using a linear regression plot (dashed line), a typical curve (dotted lines), and the theoretical EC-5 (continuous line), of the rotations, for  $\rho=150$  and  $190 \text{ kg/m}^3$ , at sections B and C (see Fig. 2) respectively.

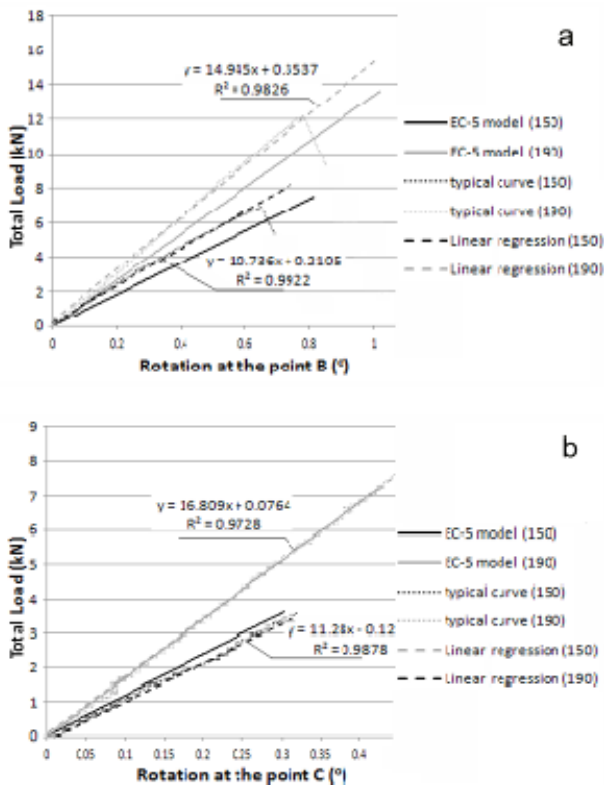


**Figure 5:** Total load (kN) versus rotation ( $^{\circ}$ ) at points B (a) and C (b), for  $\rho_{nom}=150$  and  $190 \text{ kg/m}^3$ .

### 3.6 FAILURE MODEL

The failure of the panels presented a recurring pattern, allowing the formulation of a basic failure mode. The failure is due to shear stress and starts at the WF-OSB contact surface (where the gluing process reduces the

effective section) over one support (where the shear stresses are maximum); the cracking then runs towards the centre of the beam. However, the failure surface is not a perfect plane and, even though the origin is at the glued interface, it can present some small irregularities across the section. The failure is brittle. Only one specimen failed in an unexpected way. The failure was also due to shear stress, but wasn't located at the glued interface. The reason is currently unclear; one possibility could be material irregularities. The OSB flanges did not break in any of the tests.

A failure mode considering only the maximum shear stress seems to lead to a reasonable approximation at this stage. According to this, the overall deflection and the shear stress are the two parameters to limit in the design.

### 3.7 PARAMETRICAL STUDY FOR WIND LOAD

Once the linear model was proved to fit reasonably well with the empirical data, a parametrical study was developed in order to explore the practical field of application of the proposed solution. According to the last section, two critical points were considered: a) for serviceability limit state (SLS), the midspan deflection; b) for ultimate limit state (ULS), the shear strength near the supports. Using the data from Table 1, and the model described in section 2.5, Table 2 was constructed: a typical wind load of  $1.2 \text{ kN/m}^2$  and a depth of the core ranging from 120 mm to 240 mm. The thickness of the core is mostly governed by the thermal requirements of the cladding. For German climate or similar, which was the original target of this study, calculations based on thermal conditions lead to U values between 0.15 to 0.2 ( $\text{W}/(\text{m}^2\text{K})$ ) which can be translated to an insulation depth of around 250 to 300 mm. Values in warmer regions can go down to around 120 mm [19].

**Table 2:** Maximum admissible span (m) for a simply supported (cladding) beam supporting a wind load of  $1.2 \text{ kN/m}^2$ , for both the admissible relative deflection and shear strength at the core.  $d$ =total depth (mm) considering a OSB of 15mm for every face.  $\tau$ =shear failure at the core ( $\text{N/mm}^2$ )

$\rho$	$d$	$\tau$	Failure condition: admissible relative deflection				
			1/300	1/400	1/500	1/600	1/700
110	150	1.94	2.27	1.83	1.56	1.37	1.23
	190	2.39	2.73	2.18	1.83	1.59	1.41
	230	2.86	3.20	2.54	2.12	1.83	1.61
130	270	3.35	3.68	2.92	2.42	2.08	1.82
	150	3.11	2.89	2.36	2.00	1.75	1.56
	190	3.95	3.50	2.86	2.42	2.10	1.86
150	230	4.82	4.10	3.35	2.84	2.46	2.18
	270	5.69	4.68	3.84	3.26	2.82	2.49
	150	12.3	4.14	3.64	3.27	2.98	2.75
190	15.8	4.96	4.36	3.92	3.58	3.31	
	230	19.4	5.73	5.04	4.54	4.16	3.84
	270	23.0	6.46	5.69	5.14	4.71	4.36

	150	21.8	4.45	3.97	3.62	3.35	3.13
190	190	28.1	5.31	4.74	4.33	4.01	3.75
	230	34.5	6.11	5.46	4.99	4.62	4.33
	270	40.9	6.87	6.14	5.61	5.21	4.88

The maximum span, for SLS and ULS, can be obtained from Table 2. SLS varies according to the standards and the construction system; a value from 1/300 to 1/500 is typical. Table 2 was expanded to include up to 1/700 for the possibility of increasing the global safety factor in cases where the deflection due to the hygro-thermal changes is relevant.

The viability of a solution can be determined by looking at its global safety factor, which is obtained by dividing the maximum span in ULS to the span in SLS. For example, considering  $\rho=150 \text{ kg/m}^3$ , a total depth of 270 (15+240+15) mm, and a SLS of 1/300, the global safety factor is (23m/6.46m)=3.56. As can be checked, in the typical range from 1/300 to 1/500, and  $\rho=150$  to 190  $\text{kg/m}^3$ , the global safety factor goes from a minimum of 2.97 for the core of 120mm and SLS of 1/300 to a maximum of 7.29 for the core of 240 and SLS of 1/500.

## 4 DISCUSSION

The use of timber engineering boards responds to the general search for a sustainable and environmentally friendly product. Even though there is a broad range of boards of this kind, their thickness is similar in all cases, and therefore their  $EI$  would not change substantially from one to another. The inner face can be designed with OSB because it is cost effective, the hazard class is null and in some environments it may even work without an extra vapour barrier. If an outdoor TMT or medium density fibre (MDF) board were finally used, the deflection due to hygro-thermal changes could be assumed. Other timber engineering boards, as e.g. the wood-cement boards, would also be of great interest.

It is worth checking the  $\gamma_i^*$  values (equation 1) of the real scale tested beams, for the different densities considered Table 3. As it is known,  $\gamma_i^*$  represents the reduction of the width of the WFS in order to get the equivalent current bending stiffness  $A$  value of  $\gamma_i^*=1$  means zero slip in the core, obtaining, therefore, a section with a maximum bending efficiency.

**Table 3:**  $\gamma_i^*$  value at the real scale tested beams (span = 3200 mm), for the four different densities under study

$\rho$	110	130	150	190
$\gamma_i^*$	0.09372	0.13540	0.32775	0.46571

For a density lower than 150  $\text{kg/m}^3$ , the reduction is too high, and the sandwich efficiency is greatly reduced. This confirms the range of viable core densities lies between 150 and 190  $\text{kg/m}^3$ .

The shear capacity is halved in relation with the possible maximum value due to the discontinuity of the glue

strips. This means that, according to the failure mode shown in section 3.6, the global safety factor could be doubled if the gluing surface were complete.

Both the use of TMT and WF as structural materials fit with difficulty into the scope of existing structural European standards. CE marking is now not compulsory for WFS, but can be addressed using ETAG 016 (part 3). The problem of lacking adequate EN harmonized standards for TMT and WF could thus be avoided.

## 5 CONCLUSIONS

The use of WFS for claddings made of WF with  $\rho$  ranging between 110 and 190  $\text{kg/m}^3$  was explored from a structural point of view. The WFS were designed to withstand their self weight and the wind load, and thus avoid the question of creep.

Small scale tests showed that density across a WF section is not constant. Optical measures showed that the variations between sections are negligible, and so a global and unique  $G$  value can be assumed for the overall WF section. The material behaviour of the WF lightly differs from the lower  $\rho$  (110  $\text{kg/m}^3$ ) to the upper ones (190  $\text{kg/m}^3$ ). A quasi-linear behaviour was observed for all the densities, recording that the higher the  $\rho$ , the more clear the linear behaviour.  $G_{\text{sec}}$  values were obtained for the whole range of densities, based on these small scale tests and calibrated with the real scale tests.

Real scale tests confirmed the quasi-linear behaviour of the WF core, and therefore, of the beam itself. The recorded deflections, rotations and slips at the core were compared with the linear theoretical model. The results agreed reasonably well. Small differences exist. These can be explained with the slight difference between the set up load (six point load arrangement) and the load of the theoretical model (uniformly distributed, or, at EC-5, a cosine-shape load). A further explanation is the use of a linear model for a relation that is not totally linear.

A parametrical study, using the mentioned linearized model, was carried out for the wind load. The results show that WFS is a viable solution for  $\rho$  ranging between 150 and 190  $\text{kg/m}^3$ , as the SLS can be fulfilled with a global safety factor between 3 and 8. The hygro-thermal movements do not introduce any remarkable changes to these conclusions if panels, e.g. TMT boards, with high hygro-thermal stability, are used for the outdoor flange.

This is only a preliminary study. More detailed investigations will be necessary for obtaining a commercial product.

## ACKNOWLEDGEMENT

The results presented were developed within the IP-SME project HOLIWOOD (Holistic implementation of European thermal treated hard wood in the sector of

construction industry and noise protection by sustainable, knowledge-based and value added products). This project is being carried out with financial support from the European Community within the Sixth Framework Program (NMP2-CT-2005-IP 011799-2). We would like to thank the support of the German companies Holzfaserplattenwerk H. Henselmann and Dold Holzwerke for supplying and mounting the WFS. We would also like to thank the support from GOM (Optical Measurement Techniques), and its filial Spanish company, METRONIC, and particularly to Stefan Hoheisel, for facilitating the use of the ARAMIS system. This publication reflects the authors view. The European Community and the mentioned companies are not liable for any use that may be made of the information contained therein.

## REFERENCES

- [1] ARAMIS® system. GOM mbH, Mittelweg 7-8, 38106 Braunschweig, Germany. [www.gom.com](http://www.gom.com)
- [2] Allen G, Howard (1969). Analysis and design of structural sandwich panels. Pergamon press. Oxford.
- [3] Badel E, Delisee C, Lux JSourc. (2008) 3D structural characterisation, deformation measurements and assessment of low-density wood fibreboard under compression: The use of X-ray microtomography. Composites Science and Technology 68 (7-8): 1654-1663.
- [4] Comité Européen de Normalisation (CEN) (1995) Eurocode 5 - Design of timber structures - Part 1-1: General rules and rules for buildings. ENV 1995-1-1. Bruxelles, Belgium.
- [5] Comité Européen de Normalisation (CEN). (2003) Eurocode 5 - Design of timber structures - Part 1-1: General rules and rules for buildings. prENV 1995-1-1. Bruxelles, Belgium.
- [6] Dold Holzwerke GmbH. Talstraße 9 D-79256 Buchenbach/Schwarzwald; Germany. [www.dold-holz.de/](http://www.dold-holz.de/)
- [7] Dweib MA, Hu B, O'Donnell A, Shenton HW, Wool RP (2004) All natural composite sandwich beams for structural applications. Composite Structures 63 (2):147-157.
- [8] Davis JM (Edr.) (2001) Lightweight sandwich construction. Blackwell Science.
- [9] Fernández-Cabo JL, Fernández-Lavandera J, Ávila-Jalvo JM (2008) Wood-concrete and wood-wood mixed beams: Rational basis for selecting connections. Journal of Structural Engineering-ASCE 134 (3): 440-447.
- [10] GUTEX® GUTEX Holzfaserplattenwerk H. Henselmann GmbH + Co KG, Gutenberg 5, D-79761 Waldshut-Tiengen. Germany. [www.gutex.de/](http://www.gutex.de/).
- [11] Ha KH (1990) Finite-element analysis of sandwich plates: an overview. Computers & Structures 37 (4): 397-403.
- [12] Ha KH (1992) Exact analysis of bending and overall buckling of sandwich beam systems. Computers & Structures 45 (1):31-40.
- [13] Ha KH (1993) Stiffness matrix for exact solutions of sandwich beam and frame systems. Journal of Structural Engineering-ASCE 119 (4): 1150-1167.
- [14] Kawasaki T, Zhang M, Kawai S (1998) Manufacture and properties of ultra-low-density fibreboard. J. Wood Sci. 44:354-360.
- [15] Kawasaki T, Hwang K, Komatsu K et al (2003) In-plane shear properties of the wood-based sandwich panel as a small shear wall evaluated by the shear test method using tie-rods. J. Wood Sci. 49 (3): 199-209 2003.
- [16] Kawasaki T (2006) Wood-Based Sandwich Panel with Low-Density Fiberboard for use as Structural Insulated Wall and Floor. Ph D for Graduate School of Agriculture. Research Institute for Sustainable Human sphere Kyoto University.
- [17] Kawasaki T, Kawai S (2006a) Thermal insulation properties of wood-based sandwich panel for use as structural insulated walls and floors. J. Wood Sci. 52 (1): 75-83.
- [18] Kawasaki T, Zhang M, Wang Q, Komatsu K, Kawai S (2006b) Elastic moduli and stiffness optimization in four-point bending of wood-based sandwich panel for use as structural insulated walls and floors. J. Wood Sci. 52 (4): 302-310.
- [19] Kahlert, Claus. 2008. Ein rationaler Ansatz für die Definition des Passivhauses bei gewerblicher Nutzung. Proceedings of Pasivní Domy, 2008, p. 351-356, 30.-31 Oct 2008 Brno, CZ, Jan Barta & Juraj Hazucha Editors, Centrum Pasivního Domu 2008.
- [20] NT BUILD 378:1991. Timber in structural sizes: determination of shear strength and shear modulus parallel to the grain. NORDTEST.
- [21] O'Donnell A, Dweib MA, Wool RP (2004) Natural fiber composites with plant oil-based resin. Composites Science and Technology 64 (9):1135-1145.
- [22] EOTA: Organisation for Technical Approvals. Ed. February 2005. ETAG-016. Self-supporting composite lightweight panels. PART 3:Specific aspects relating to Self-supporting composite lightweight panels for use in external walls and claddings.
- [23] Poquillon D, Viguier B, Andrieu E (2005) Experimental data about mechanical behaviour during compression tests for various matted fibres. Journal of materials science 40 (22): 5963-5970 NOV 2005.
- [24] Pourdeyhimi B, Maze B, Tafreshi HV (2006) Simulation and analysis of unbonded nonwoven fibrous structures. Journal of engineered fibers and fabrics 1 (2): 47-65 2006
- [25] Wada A, Kawasaki T, Minoda Y, Kataoka A, Tashiro S, Fukuda H (2003) A method to measure shearing modulus of the foamed core for sandwich plates. Composite Structures 60: 385-390